

## Parton distributions for the octet and decuplet baryons

C. Boros and A. W. Thomas

*Department of Physics and Mathematical Physics, and Special Research Center for the Subatomic Structure of Matter,  
University of Adelaide, Adelaide 5005, Australia*

(Received 17 February 1999; published 8 September 1999)

We calculate the parton distributions for both polarized and unpolarized octet and decuplet baryons, using the MIT bag, dressed by mesons. We show that the hyperfine interaction responsible for the  $\Delta$ - $N$  and  $\Sigma^0$ - $\Lambda$  splittings leads to large deviations from  $SU(3)$  and  $SU(6)$  predictions. For the  $\Lambda$  we find significant polarized, non-strange parton distributions which lead to a sizable  $\Lambda$  polarization in polarized, semi-inclusive  $ep$  scattering. We also discuss the flavor symmetry violation arising from the meson cloud associated with the chiral structure of baryons. [S0556-2821(99)06417-6]

PACS number(s): 14.20.-c, 11.30.Hv, 12.39.Ba

### I. INTRODUCTION

Parton distributions contain valuable information on the non-perturbative structure of hadrons. An impressive amount of data for both polarized and unpolarized structure functions on nucleon targets has been collected over the past two decades. However, relatively less is known about the parton distributions in other baryons. Measurements of parton distributions for members of the baryon octet would give us complementary information to that obtained from the nucleon and could shed light on many phenomena involving non-perturbative QCD, such as  $SU(3)$  symmetry breaking, the flavor asymmetry in the nucleon sea and so on.

Experimentally it should be possible to access the parton distributions of  $\Sigma^+$  hyperons through the Drell-Yan process. Furthermore, since the  $\Sigma$ 's are in general polarized because of their production mechanism, it should also be possible, in principle, to measure the polarized quark distributions in sigma hyperons.

It was recently pointed out by Alberg *et al.* [1] that the mechanism responsible for the splitting of the  $\Delta$ - $N$  and  $\Sigma^0$ - $\Lambda$  masses could lead to considerable  $SU(3)$  symmetry breaking in the parton distributions among members of the baryon octet. Here, we show explicitly that this is indeed the case by calculating the quark distribution of baryons in the MIT bag model, where we include the hyperfine interaction which leads to the splitting of the baryon masses. The  $SU(3)$  breaking which we find goes beyond the implicit breaking of  $SU(3)$  by the strange quark mass, since it leads to deviations from  $SU(3)$  expectations even among baryons with the same number of strange (valence) quarks. We also investigate the influence of the meson cloud on the shape of the "bare" quark distributions and calculate the flavor asymmetries in the sea arising from the meson-baryon fluctuations.

### II. BARE QUARK DISTRIBUTIONS

#### A. Baryon octet

The starting point of our calculation is the general expression for the quark distribution in a baryon  $B$  with mass  $m$  [2,3]:

$$q_f(x) = \frac{m}{(2\pi)^3} \sum_n \int d^3p_n |\langle n; \mathbf{p}_n | \psi_+(0) | B \rangle|^2 \times \delta[(1-x)m - p_n^+]. \quad (1)$$

Here  $\psi_+ = \frac{1}{2} \gamma_- \gamma_+ \psi$  is the plus projection of the quark field operator, the states  $|n; \mathbf{p}_n\rangle$  are intermediate states with mass  $m_n$  and form a complete set of states with  $p_n^+ = \sqrt{m_n^2 + \mathbf{p}_n^2} + p_{nz}$ . We stress that Eq. (1) assures the correct support for  $q_f(x)$ , regardless of the approximations made for  $|n; \mathbf{p}_n\rangle$  and  $|B\rangle$ . The operator  $\psi$  either destroys a quark in the initial state leaving a two quark system in the intermediate state or it creates an antiquark. Concentrating on the two quark intermediate states, and using MIT bag wave functions and the Peierls-Yoccoz method for constructing approximate momentum eigenstates, the spin-dependent parton distributions take the form [3,4]

$$q_f^{\uparrow\downarrow}(x) = \frac{m}{(2\pi)^2} \sum_m \langle B | P_{f,m} | B \rangle \times \int_{[m^2(1-x)^2 - m_n^2]/2m(1-x)}^{\infty} \times p_n dp_n \frac{|\phi_2(\mathbf{p}_n)|^2}{|\phi_3(\mathbf{0})|^2} |\Psi_m^{\uparrow\downarrow}(\mathbf{p}_n)|^2. \quad (2)$$

Here  $|\phi_2(\mathbf{p}_n)|^2$  and  $|\phi_3(\mathbf{0})|^2$  originate from the Peierls-Yoccoz projections of the two quark intermediate states and the (three quark) baryon, respectively.  $\langle B | P_{f,m} | B \rangle$  projects out the appropriate quantum numbers from the spin-flavor wave function of the initial state.  $\Psi_m^{\uparrow\downarrow}(\mathbf{p}_n)$  are the Fourier transforms of the helicity and plus component projections,  $\Psi^{\uparrow\downarrow}(\mathbf{x}) = \frac{1}{2} \gamma_- \gamma_+ \frac{1}{2} (1 \pm \gamma_5) \Psi_m(\mathbf{x})$ , of the MIT bag wave function

$$\Psi_m(\mathbf{x}) = N(\Omega) \begin{pmatrix} \sqrt{\frac{\omega + m_q}{\omega}} j_0\left(\frac{\Omega|\mathbf{x}|}{R}\right) \chi_m \\ i \sqrt{\frac{\omega - m_q}{\omega}} (\boldsymbol{\sigma} \cdot \hat{\mathbf{x}}) j_1\left(\frac{\Omega|\mathbf{x}|}{R}\right) \chi_m \end{pmatrix} \Theta(R - |\mathbf{x}|) \quad (3)$$

with frequency  $\omega = \sqrt{\Omega^2 + (m_q R)^2}/R$ , bag radius  $R$  and normalization constant  $N(\Omega)$ .  $\Omega$  is the solution of the eigenvalue equation  $\tan(\Omega) = \Omega/(1 - mR - \sqrt{\Omega^2 + (mR)^2})$ .

As we have already noted, the advantage of using Eq. (1) is that energy-momentum conservation is ensured and thus the quark distributions obtained from it have correct support.<sup>1</sup> The delta function implies that the distribution peaks at  $x \approx (1 - m_n/m)$ , introducing a dependence of the shape of the quark distributions on the mass of the intermediate systems,  $m_n$ . Although intermediate states with higher number of quarks are possible, these contributions peak at negative  $x$  values ( $m_n > m$ ) giving only a small contribution in the physical  $x$ -region. Thus, the main contribution for larger  $x$  values comes from spectator systems with two quarks. Since the hyperfine interaction responsible for the splitting of the  $\Delta$ - $N$  masses also splits the masses of scalar and vector diquarks and whether the struck quark is accompanied by a scalar or vector diquark is flavor dependent, this splitting leads to flavor dependent distortions in the shape of the quark distributions compared to exact  $SU(6)$  symmetry. In the case of the nucleons, the  $u$ -quark distribution peaks at larger  $x$ -values than the  $d$ -quark distribution. These arguments for the explanation of the observed  $SU(6)$  violation in the quark distributions of the proton were first discussed in Ref. [5] and later implemented in the calculation of quark distributions in the MIT bag model for the proton [3,4]. The same arguments can be applied to other baryons.

It is instructive to review the mass-splitting of the baryons here. The exact mechanism for this splitting is not essential for the calculation of the quark distribution since only the masses of the scalar and vector diquarks enter the calculation and different mechanisms/explanations lead to similar results. However, in order to illustrate how these numbers are obtained we discuss the one-gluon exchange model.

The color hyperfine interaction Hamiltonian is given by

$$H_{hf} = -\frac{1}{4} \sum_{i < j} v(m_i, m_j) (\vec{\sigma}_i \cdot \vec{\sigma}_j) \lambda_i^a \lambda_j^a \quad (4)$$

with  $\frac{1}{2} \vec{\sigma}_i$  the spin of quark  $i$  and  $\lambda_i^a$  the corresponding color matrix. The strength of the interaction depends, in general, on the mass of the quarks. This dependence is taken care of by  $v(m_i, m_j)$  in Eq. (4). The sum over the color matrices can be calculated. One obtains  $-\frac{16}{3}$  for quark-antiquark pairs and  $-\frac{8}{3}$  for baryons.

Attributing the entire mass splitting between the nucleon and the  $\Delta$  to the hyperfine interaction, the splitting is given by  $\langle H_{hf} \rangle$ . For three quarks, the spin sum in Eq. (4) is  $\sum_{i < j} (\vec{\sigma}_i \cdot \vec{\sigma}_j) = (\vec{\sigma}_1 + \vec{\sigma}_2) \cdot \vec{\sigma}_3 + \vec{\sigma}_1 \cdot \vec{\sigma}_2$ . For a spin-0 and spin-1 diquark state, we have  $\langle \vec{\sigma}_1 \cdot \vec{\sigma}_2 \rangle_{S=0} = -3$  and  $\langle \vec{\sigma}_1 \cdot \vec{\sigma}_2 \rangle_{S=1} = 1$ , respectively. Thus, one gluon exchange is attractive for scalar diquarks and repulsive for vector di-

quarks. Coupling the remaining quark to the spin-triplet diquark state one obtains  $\langle \vec{\sigma}_3 \cdot (\vec{\sigma}_1 + \vec{\sigma}_2) \rangle = -4$  for the nucleon and  $\langle \vec{\sigma}_3 \cdot (\vec{\sigma}_1 + \vec{\sigma}_2) \rangle = 2$  for the  $\Delta$ . Thus, the shifts in the nucleon and  $\Delta$  masses are given by  $\Delta m_N = -2 v(m_u, m_u)$  and  $\Delta m_\Delta = 2 v(m_u, m_u)$ , respectively, and the total splitting between the  $\Delta$  and the nucleon is  $\Delta M = 4 v(m_u, m_u)$ . Since  $\Delta M$  is  $\approx 300$  MeV we have  $v(m_u, m_u) \approx 75$  MeV. The nucleon and the  $\Delta$  would be degenerate at  $m = M_\Delta - 2 v(m_u, m_u) \approx (1230 - 150)$  MeV = 1080 MeV, without hyperfine splitting. Further, we see that the triplet diquark is heavier by 50 MeV and the singlet diquark is lighter by 150 MeV than the diquark state without hyperfine interaction.

The same arguments applied to the  $\Lambda$  and  $\Sigma$  lead to the following equations:

$$\begin{aligned} \Delta_\Lambda &= \frac{2}{3} v(m_u, m_u) (-3) = -150 \text{ MeV} \\ \Delta_\Sigma &= \frac{2}{3} \{ v(m_u, m_u) - 4 v(m_u, m_s) \}. \end{aligned} \quad (5)$$

Thus, for  $v(m_u, m_s)$  we obtain, with  $m_\Sigma - m_\Lambda = \Delta m_\Sigma - \Delta m_\Lambda$

$$v(m_u, m_s) = v(m_u, m_u) - \frac{3}{8} (m_\Sigma - m_\Lambda) \approx 46 \text{ MeV}. \quad (6)$$

$\Lambda$  and  $\Sigma$  would be degenerate with a mass of  $\approx 1260$  MeV without hyperfine interactions. The  $us$  vector diquark is heavier by  $\frac{2}{3} v(m_u, m_s) \approx 30$  MeV and the corresponding scalar diquark is lighter by  $2 v(m_u, m_s) \approx 90$  MeV than the diquark without hyperfine splitting.

The mass of a diquark containing only  $u$  and  $d$  quarks is about  $\frac{3}{4}$  of the degenerate mass of the nucleon and the  $\Delta$ , which is roughly 800 MeV. This gives us the masses  $m_s = 650$  MeV and  $m_v = 850$  MeV for triplet and singlet diquarks containing  $u$  and  $d$  quarks. To estimate the masses of diquarks containing a strange quark and an up or down quark we use the phenomenological fact that the strange quark adds about 180 MeV. Thus, we have  $m'_s = 800 + 180 - 90 \approx 890$  MeV and  $m'_v = 800 + 180 + 30 = 1010$  MeV for singlet and triplet diquarks.

Having obtained the masses of the various diquark states, we turn our attention to the quark distributions in different baryons. One of the consequences of the mass differences between scalar and vector diquarks is that the up quark distribution in the proton peaks at larger  $x$ -values than the down quark distribution. To see this we note that the  $SU(6)$  wave function of the proton is

$$\begin{aligned} p^\uparrow &= \frac{1}{3\sqrt{2}} [3u^\uparrow(ud)_{0,0} + u^\uparrow(ud)_{1,0} - \sqrt{2}u^\uparrow(ud)_{1,1} \\ &\quad - \sqrt{2}d^\uparrow(uu)_{1,0} + 2d^\uparrow(uu)_{1,1}]. \end{aligned} \quad (7)$$

Here, we use the notation  $(qq)_{S,S_z}$  for the diquark spin states with  $S$  and  $S_z$  the total spin and spin projection of the diquarks. While only vector diquarks enter the calculation of

<sup>1</sup>Note that this is guaranteed by Eq. (1) regardless of the approximation used for the states  $|n; \mathbf{p}_n\rangle$  and  $|B\rangle$ —in this case a Peierls-Yoccoz projection.

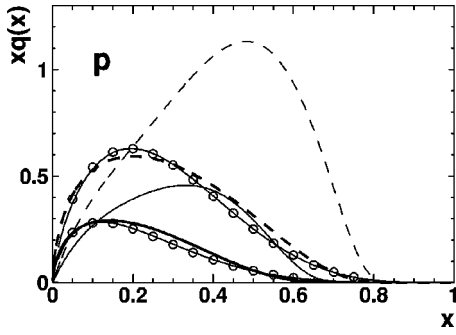


FIG. 1. The up (dashed lines) and down (solid lines) valence quark distribution in the proton at  $Q^2 = \mu^2 = 0.23 \text{ GeV}^2$  (light lines) and  $Q^2 = 10 \text{ GeV}^2$  (heavy lines). The quark distributions at  $Q^2 = 10 \text{ GeV}^2$  already include the meson-cloud corrections. The Cteq4M distributions representing the “data” are shown as solid lines with open circles.

the down quark distribution, both vector and scalar diquarks are relevant for the up quark distribution in the proton, with the scalar diquark having a much larger probability. According to the  $\delta$  function in Eq. (1) the distribution of quarks accompanied by scalar diquarks, here the up quark distribution, should peak around  $x = 1 - m_s/m = 1 - 650/940 \approx 0.31$  and that associated with a vector diquark, here the down quark distribution, around  $x = 1 - m_v/m = 1 - 850/940 \approx 0.1$  — at the scale relevant for the bag model.

The implementation of these ideas is discussed in Ref. [4] in detail. Here, we only note that the Fourier transform of the wave function in Eq. (2) can be split into a spin dependent and a spin independent part:

$$|\Psi_m^{\uparrow\downarrow}(\mathbf{p}_n)|^2 = \frac{1}{2} [f(\mathbf{p}_n) \pm (-1)^{m+3/2} g(\mathbf{p}_n)]. \quad (8)$$

Since one uses a fixed polarization axis in the bag model the helicity states have to be projected out from the bag wave function and thus both polarization states,  $m = \pm \frac{1}{2}$ , contribute to a given helicity projection,  $\uparrow$  or  $\downarrow$ . The expressions for  $f(\mathbf{p}_n)$ ,  $g(\mathbf{p}_n)$  and also for the Peierls-Yoccoz projections  $|\phi_2(\mathbf{p}_n)|^2$  and  $|\phi_3(\mathbf{0})|^2$  can be found in Ref. [4] for massless quarks. The generalization to massive quarks is straightforward (multiplication of those parts of the expressions which comes from the upper and lower components by  $\sqrt{(\omega \pm m_q)/\omega}$ , respectively and using the normalization constant of the wave function for massive quarks).

Denoting by  $F(x)$  and  $G(x)$  those contributions to Eq. (2) which come from the  $f(\mathbf{p}_n)$  and  $g(\mathbf{p}_n)$  parts of the integral and using the wave function of the proton [Eq. (7)] to calculate the projections  $\langle B | P_{f,m} | B \rangle$ , we obtain

$$u^{\uparrow\downarrow}(x) = \frac{1}{4} [F_v(x) + 3F_s(x)] \mp \frac{1}{12} [G_v(x) - 9G_s(x)],$$

$$d^{\uparrow\downarrow}(x) = \frac{1}{2} F_v(x) \mp \frac{1}{6} G_v(x). \quad (9)$$

Here, the subscripts,  $s$  and  $v$ , on  $F(x)$  and  $G(x)$  indicate whether the intermediate states are scalar or vector diquarks.

We calculated the quark distributions using 0.8 fm for the bag radius;  $m_v = 850 \text{ MeV}$  and  $m_s = 650 \text{ MeV}$  for the vector and scalar diquark masses. The result is shown in Fig. 1 as light lines for a starting scale  $\mu^2 = 0.23 \text{ GeV}^2$ . As discussed in Ref. [4], the two-quark intermediate states alone do not saturate the normalization of the quark distributions. There are also contributions from four quark intermediate states which have to be taken into account when normalizing the distributions. Since these peak at negative  $x$ -values due to the larger mass of the intermediate states, they give rise to distributions which drop fast in the physical  $x$ -region. Here, we use the procedure adopted in the original paper [4] and parametrize the four-particle contributions in the form  $(1-x)^7$  (which gives an excellent approximation to the actual shape of the distributions) such that the normalization is satisfied. After evolving the distributions to  $Q^2 = 10 \text{ GeV}^2$  (heavy lines) we find a good agreement between the calculated distributions and the experimental data which is represented by the CTEQ4M parametrization of the quark distributions [6]. The results at  $Q^2 = 10 \text{ GeV}^2$  already contain corrections from the meson-cloud which will be discussed later. The quark distributions have been evolved in next leading order (NLO) with  $\Lambda_{QCD} = 0.225 \text{ GeV}$  and four active flavors, using the package of Ref. [7].

Now, having fixed the parameters, let us generalize these arguments to the  $\Sigma^+$ . (This extension was first investigated semi-quantitatively in Ref. [1].) The wave function of the  $\Sigma^+$  is given by Eq. (7) with the  $d$ -quark replaced by an  $s$ -quark. (N.B. There must be a phase factor  $-1$  relative to that of proton wave function, in order to match the phase convention of de Swart [8] which we use.) The distribution of the strange quarks is determined by the mass of the vector  $uu$ -diquark. It peaks at  $x = 1 - m_v/m_\Sigma = 1 - 850/1190 \approx 0.29$ , which is close to the value found for the up quark distribution in the proton. The maximum of the  $u_\Sigma$  quark distribution is determined by the masses of both the  $us$  scalar and vector diquarks, which are  $\approx 890 \text{ MeV}$  and  $1010 \text{ MeV}$ , respectively. Thus,  $x = 1 - m'_s/m_\Sigma = 1 - 890/1190 \approx 0.25$  for the scalar diquark and  $x = 1 - m'_v/m_\Sigma = 1 - 1010/1190 \approx 0.15$  for the vector diquark, which are both smaller than the corresponding values for  $u_p$  and  $s_\Sigma$ . For the quark distributions we have, similar to Eq. (9),

$$u_{\Sigma^+}^{\uparrow\downarrow}(x) = \frac{1}{4} [F'_v(x) + 3F'_s(x)] \mp \frac{1}{12} [G'_v(x) - 9G'_s(x)],$$

$$s_{\Sigma^+}^{\uparrow\downarrow}(x) = \frac{1}{2} F'_v(x) \mp \frac{1}{6} G'_v(x). \quad (10)$$

Here,  $F'(x)$  and  $G'(x)$  differ from  $F(x)$  and  $G(x)$  because they are calculated by using the appropriate masses of the heavy diquarks and taking into account that one of the spectator quarks is massive when making the Peierls-Yoccoz projections. In the calculation of  $s(x)$  the struck quark is massive and the spectator quarks are massless. Thus, we calculate the Fourier transform  $\Psi^{\uparrow\downarrow}(\mathbf{p}_n)$  with the quark mass  $m_q = 180 \text{ MeV}$  and the Peierls-Yoccoz projections,  $|\phi_2(\mathbf{p}_n)|^2$ , with massless quarks. The results for the unpolar-

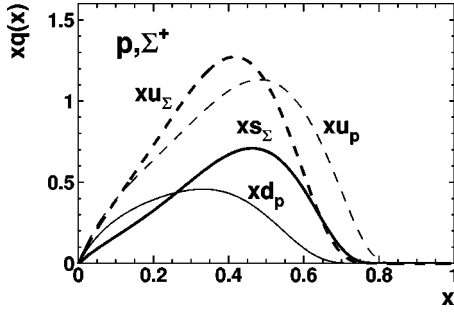


FIG. 2. The strange (heavy solid line) and up (heavy dashed line) valence quark distributions in  $\Sigma^+$  compared to the down (light solid line) and up (light dashed line) quark distributions in the proton—all evaluated at the bag scale,  $\mu^2$ .

ized and polarized distributions are shown in Fig. 2 and Fig. 3 (heavy lines) together with the results for the proton (light lines). We see a considerable difference from the  $SU(3)$  expectations,  $s_\Sigma = d_p$  and  $u_\Sigma = u_p$ .

The ratio  $r_\Sigma \equiv s_\Sigma / u_\Sigma$  is shown in Fig. 4 for both the bare quark distributions (solid line) and the distributions dressed by mesons (dashed line). We see that  $r_\Sigma$  increases for  $x \rightarrow 1$  in contrast with  $SU(3)$  expectations which predict a behavior similar to that of  $d/u$  in the proton. [The  $SU(3)$  expectation,  $r_{SU(3)} = r_p = d_p / u_p$ , is shown as the dotted line.] Exact  $SU(6)$  symmetry would predict a constant ratio, independent of  $x$ , and this is shown as solid line in Fig. 4. We stress that these  $SU(3)$  violations come partly through the explicit  $SU(3)$  breaking by the strange quark mass and partly through the hyperfine interaction.  $SU(3)$  breaking through the strange mass alone would not split the mass of the  $\Lambda$  and  $\Sigma$  hyperons and would lead to identical parton distributions in these hyperons. However, this is not the case and the hyperfine interaction plays a decisive role in the shape of the parton distributions of the hyperons.

The quark distributions of the  $\Lambda$  and  $\Sigma^0$  hyperons are interesting by themselves but we also need them to calculate the corrections arising from the meson-cloud later. The  $SU(6)$  wave function of the  $\Sigma^0$  hyperon with given positive polarization is

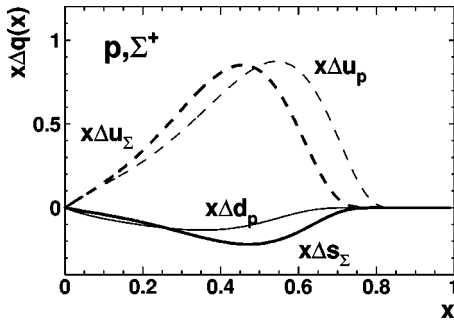


FIG. 3. The polarized strange  $x\Delta s(x) = xs^\uparrow(x) - xs^\downarrow(x)$  (heavy solid line) and up  $x\Delta u(x)$  (heavy dashed line) valence quark distributions in the  $\Sigma^+$ , compared to the polarized down (light solid line) and up (light dashed line) quark distributions in the proton (at the bag scale,  $\mu^2$ ).

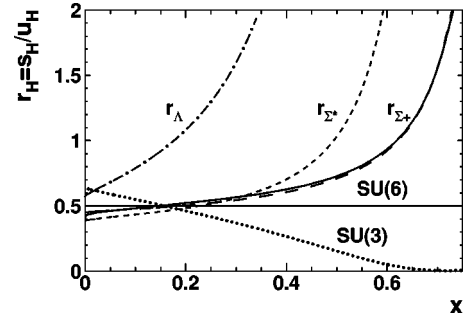


FIG. 4. The ratios  $r_H \equiv s_H / u_H$  for different baryons, after evolving the quark distributions to  $Q^2 = 10 \text{ GeV}^2$ . The ratio  $r_{\Sigma^+} \equiv s_{\Sigma^+} / u_{\Sigma^+}$  is shown as the solid and dashed lines, with and without meson-cloud corrections, respectively. The  $SU(3)$  expectation, which corresponds to  $r_\Sigma = \frac{1}{2} r_\Lambda = r_p = d_p / u_p$ , is shown as a dotted line.  $SU(6)$  would give a constant ratio of 1/2, independent of  $x$  (solid line), and is realized for the decuplet baryons containing only massless quarks ( $\Delta^+$ ). However, it is broken for the decuplet hyperons (short dashed line)—see Sec. II B.

$$\begin{aligned} \Sigma^{0\uparrow} = & \frac{1}{3\sqrt{2}} \left[ \sqrt{2}s^\uparrow(ud)_{1,0} - 2s^\downarrow(ud)_{1,1} - \frac{1}{\sqrt{2}}d^\uparrow(us)_{1,0} \right. \\ & + d^\downarrow(us)_{1,1} - \frac{3}{\sqrt{2}}d^\uparrow(us)_{0,0} - \frac{1}{\sqrt{2}}u^\uparrow(ds)_{1,0} + u^\downarrow(ds)_{1,1} \\ & \left. - \frac{3}{\sqrt{2}}u^\uparrow(ds)_{0,0} \right]. \end{aligned} \quad (11)$$

The  $ud$  diquark is always a vector diquark so that the maximum of the distribution of the strange quark is determined only by the mass of the vector diquarks. Comparing with the wave function of the  $\Sigma^+$  we see that  $u_{\Sigma^0} = d_{\Sigma^0} = \frac{1}{2}u_{\Sigma^+}$  and  $s_{\Sigma^0} = s_{\Sigma^+}$ .

On the other hand, the  $SU(6)$  wave function of the  $\Lambda$  hyperon is

$$\begin{aligned} \Lambda^\uparrow = & \frac{1}{2\sqrt{3}} [2s^\uparrow(ud)_{0,0} + \sqrt{2}d^\downarrow(us)_{1,1} - d^\uparrow(us)_{1,0} + d^\downarrow(us)_{0,0} \\ & - \sqrt{2}u^\downarrow(ds)_{1,1} + u^\uparrow(ds)_{1,0} - u^\downarrow(ds)_{0,0}]. \end{aligned} \quad (12)$$

Whereas the maximum of the  $u$  and  $d$  distributions is determined by both the vector and scalar diquark masses, only the mass of the scalar diquark is relevant for the maximum of the distribution of the  $s$ -quark.  $s_\Lambda$  peaks at  $x = 1 - 650/1115 \approx 0.42$ . This yields a very hard distribution. For the  $u$  and  $d$  distributions we find that the peaks of the valence distributions should occur around  $x = 1 - 890/1115 \approx 0.20$  and  $x = 1 - 1010/1115 \approx 0.10$  for scalar and vector diquarks, respectively. The quark distributions of the  $\Lambda^\uparrow$  are given by

$$\begin{aligned} u_\Lambda^{\uparrow\downarrow}(x) = d_\Lambda^{\uparrow\downarrow}(x) = & \frac{1}{8} [3F'_v(x) + F'_s(x)] \mp \frac{1}{8} [G'_v(x) - G'_s(x)] \\ s_\Lambda^{\uparrow\downarrow}(x) = & \frac{1}{2} [F_s(x) \pm G_s(x)]. \end{aligned} \quad (13)$$

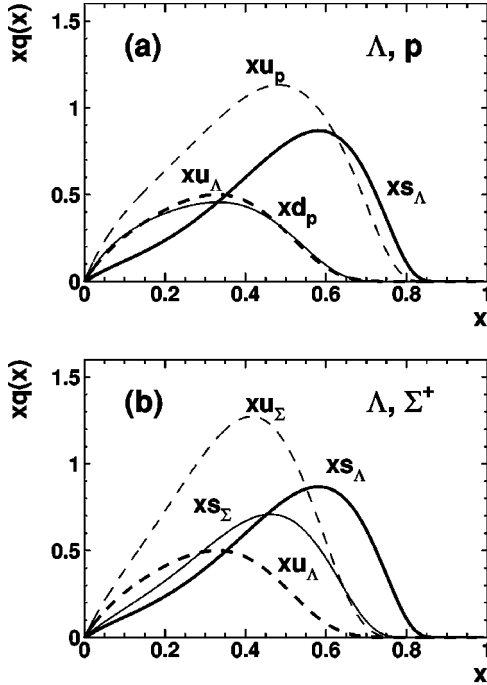


FIG. 5. Quark distributions in the  $\Lambda$  compared to the quark distribution (a) in the proton and (b) in the  $\Sigma^+$ —at the bag scale,  $\mu^2$ .

The results are shown in Fig. 5 and Fig. 6 for the polarized and unpolarized distributions compared to the corresponding distribution in other baryons. The strange quark distribution in the  $\Lambda$  is much harder than the corresponding strange quark distributions in the  $\Sigma^+$  and  $\Sigma^0$ . Large deviations from  $SU(3)$  expectations are most evident in Fig. 4, where the ratio  $r_\Lambda \equiv s_\Lambda/u_\Lambda$ , shown as the dash-dotted line, is compared to the corresponding ratios in other hyperons. Exact  $SU(6)$  would give  $r_\Lambda = 1$  and  $SU(3)$   $r_\Lambda = 2r_p \equiv 2d_p/u_p$ .

A naive approach to take into account the  $SU(3)$  breaking would be to choose larger masses for strange quarks than for the up and down quarks and to argue that the strange quark distributions should peak at higher  $x$ -values than the light quark distributions due to its higher mass. Then, we would still obtain  $u_\Lambda = d_\Lambda = \frac{1}{2}u_\Sigma$  and  $s_\Lambda = s_\Sigma$ . However, this

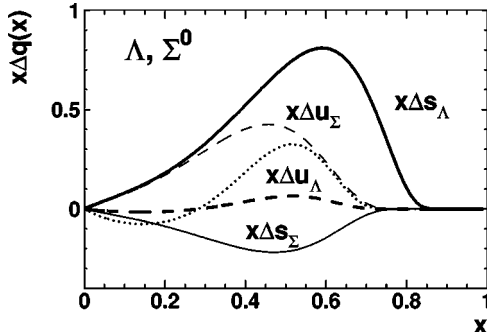


FIG. 6. Polarized quark distributions in the  $\Sigma^0$  and the  $\Lambda$  at the bag scale,  $\mu^2$ . The dotted line stands for five times  $x\Delta u_\Lambda$  and indicates the relative importance of the  $u$  and  $d$  quarks in  $g_1$ .

is not the case as can be seen in Figs. 5 and 6. We also see that, in contrast to the static quark model, the strange quark does not carry the total spin of the  $\Lambda$  in the bag model, due to its transverse motion in the bag. Although the total contribution of the  $u$  and  $d$  quarks to the spin of the  $\Lambda$  (i.e. the integral over  $\Delta u_\Lambda$  and  $\Delta d_\Lambda$ ) is zero, the net polarization for given  $x$  is non-vanishing. The splitting of the scalar and vector diquark masses shifts the light quark distributions with the same polarization as the  $\Lambda$  to higher  $x$ -values with respect to the corresponding distributions with opposite polarization. If  $G'_v$  and  $G'_s$  had the same form,  $\Delta u(x) = \frac{1}{2}(G'_s(x) - G'_v(x))$  would be zero.  $\Delta u(x)$  and  $\Delta d(x)$  are positive for large  $x$  and negative for smaller  $x$  values (see Fig. 6).

It should be possible to test these results for the shapes of  $\Delta u(x)$  and  $\Delta d(x)$  in semi-inclusive deep inelastic scattering with longitudinally polarized electrons. Here, the smallness of the  $u$  and  $d$  polarizations relative to the strange quark polarization is compensated by the abundance of  $u$ -quarks in the valence region and by the fact that  $s$  quarks are suppressed by a factor of  $1/9$  compared to the corresponding factor of  $4/9$  for the  $u$ -quark in electromagnetic interactions. (In Fig. 6 we show five times  $\Delta u(x)$  as a dotted line to indicate the relative magnitude of the contribution of  $u$  and  $d$  to  $g_1^\Lambda$ .)  $\Lambda$ 's produced in the current fragmentation region are mainly fragmentation products of  $u$ -quarks. Part of the polarization of the electron is transferred to the struck quark in the scattering process. This polarization will be transferred to the final  $\Lambda$  if the helicity dependent fragmentation functions,  $\Delta D_u^\Lambda$  are non-zero [9]. Since, according to the above discussion, the  $u$  and  $d$  quarks in the  $\Lambda$  hyperon may be polarized at a fixed Bjorken  $x$ , we expect on general grounds that polarized  $u$  and  $d$ -quarks may also fragment into a polarized  $\Lambda$ -hyperon. In fact, as pointed out by Gribov and Lipatov [10], the fragmentation function  $D_q^h(z)$ , for a quark  $q$  splitting into a hadron  $h$  with longitudinal momentum fraction  $z$ , is related to the quark distribution  $q_h(x)$ , for finding the quark  $q$  inside the hadron  $h$  carrying a momentum fraction  $x$ , by the reciprocity relation

$$D_q^h(z) \sim q_h(z) \quad (14)$$

for  $z \sim 1$ . Despite the limited range of validity of this relation, Eq. (14) can serve as a first estimate of the fragmentation function [11]. Since  $\Delta q_z^\Lambda$  is positive for large  $x$  we expect to find positive polarization for  $\Lambda$ 's produced in the current fragmentation region. This is the opposite of the prediction of Jaffe [9], based on  $SU(3)$  symmetry.

In order to estimate the expected  $\Lambda$  polarization, we note that the polarization for the scattering of polarized electrons off an unpolarized target  $N$  is given by [9]

$$\tilde{P}_\Lambda = \hat{e}_3 P_e \frac{y(2-y)}{1+(1-y)^2} \frac{\sum_q e_q^2 q_N(x, Q^2) \Delta D_q^\Lambda(z, Q^2)}{\sum_q e_q^2 q_N(x, Q^2) D_q^\Lambda(z, Q^2)}, \quad (15)$$

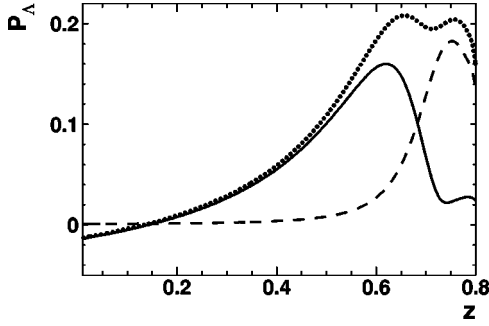


FIG. 7. The polarization of the  $\Lambda$  produced in semi-inclusive, polarized  $e$ - $p$  scattering, with the electron polarization arbitrarily set to 50%. The contributions from the fragmentation of  $u$  and  $s$  quarks are shown as solid and dashed lines, respectively. The dotted line is the total polarization.

where  $y \equiv (E - E')/E$  is the usual deep inelastic scattering (DIS) variable; the electron beam defines the  $\hat{e}_3$  axis and  $P_e$  is the degree of polarization of the incident electron.  $P_\Lambda$  measures  $\Delta D_u^\Lambda / D_u^\Lambda$  for not too small Bjorken- $x$  values, where the contributions from the strange quarks may be neglected. We calculated the  $\Lambda$  polarization using  $\Delta D_u^\Lambda = \Delta D_d^\Lambda$  and the reciprocity relation to replace the fragmentation functions by the quark distribution functions. The result calculated at  $E_e \approx 30$  GeV,  $x = 0.3$  and  $Q^2 = 10$  GeV<sup>2</sup>, where  $y = 0.58$ , is shown in Fig. 7. We assumed a beam polarization of 50%. The solid and dashed lines are the contributions from the fragmentation of  $u$ -quarks and  $s$ -quark, respectively. The dotted line is the total polarization. The contribution of the  $u$ -quarks dominates at  $x \sim 0.5$ . Since the  $s$ -quark distribution in  $\Lambda$  peaks at larger  $x$ -values than the  $u$ -quark distribution, we also predict  $D_u^\Lambda / D_s^\Lambda \rightarrow 0$  for  $z \rightarrow 1$  for the fragmentation functions and, thus, the contribution of  $s$ -quarks to  $P_\Lambda$  eventually dominates at very large  $z$ . However, since the cross section decreases rapidly with increasing  $z$ , the bulk of the produced  $\Lambda$ 's are fragmentation products of  $u$ -quarks. Thus,  $P_\Lambda \neq 0$  at not too large  $z$  will test our prediction.

### B. Baryon decuplet

Although the quark distributions of baryons from the baryon decuplet are unlikely to be measured in the near future they are of interest when we calculate the corrections associated with meson-baryon fluctuations.

First of all let us check whether the values of  $v(m_u, m_u)$  and  $v(m_u, m_s)$  obtained from the  $\Delta$ - $N$  and  $\Lambda^0$  and  $\Sigma^0$  splittings are consistent with the values from the splitting of the  $\Sigma$  and  $\Sigma^*$  baryons. The masses of the  $\Sigma^+$  and  $\Sigma^{*+}$  are shifted by

$$\begin{aligned} \Delta m_{\Sigma^+} &= \frac{2}{3} [v(m_u, m_u) - 4v(m_u, m_s)] \\ \Delta m_{\Sigma^{*+}} &= \frac{2}{3} [v(m_u, m_u) + 2v(m_u, m_s)] \end{aligned} \quad (16)$$

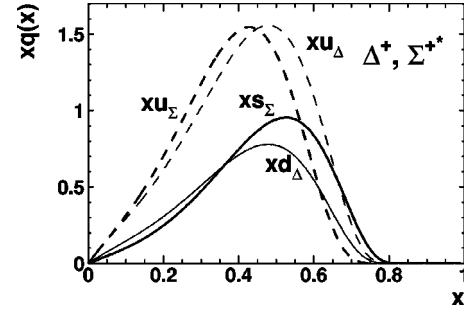


FIG. 8. Quark distributions in the  $\Delta^+$  and  $\Sigma^{*+}$  at the bag scale,  $\mu^2$ .

with respect of the degenerate mass. Thus, the mass difference  $m_{\Sigma^{*+}} - m_{\Sigma^+} = 4v(m_u, m_s)$  gives  $v(m_u, m_s) \approx 48$  MeV which is very close to the value  $v(m_u, m_s) \approx 46$  MeV obtained from the  $\Lambda^0$ - $\Sigma^0$  splitting.

Since the baryons in the decuplet are spin-3/2 particles, the spectator diquark system is always a vector diquark independent of the flavor of the struck quark and of the type of baryon. This has the important consequence that the distributions of quarks of different flavor all have the same shape in the  $\Delta$ -baryons. Thus,  $SU(6)$  is a good symmetry for the  $\Delta$  baryons. The distributions have a maximum at  $x = 1 - m_v/m_\Delta \approx 0.31$  which is harder than the  $d$ -quark distribution in the proton, because of the larger mass of the  $\Delta$ , but somewhat softer than the distribution of the  $u$ -quarks in the proton. Let us take the  $\Delta^+$  as a representative for the  $\Delta$  baryons and denote the spin projections  $\pm \frac{1}{2}$  by  $\uparrow\downarrow$  and  $\pm \frac{3}{2}$  by  $\uparrow\uparrow$ . The  $SU(6)$  wave function of  $\Delta^{+\uparrow}$  may be written as

$$\begin{aligned} \Delta^{+\uparrow} &= \frac{1}{3} [d^\downarrow(uu)_{1,1} + \sqrt{2}d^\uparrow(uu)_{1,0} + \sqrt{2}u^\downarrow(ud)_{1,1} \\ &\quad + 2u^\uparrow(ud)_{1,0}]. \end{aligned} \quad (17)$$

The quark distributions of the  $\Delta^{+\uparrow}$  are then given by

$$\begin{aligned} u_{\Delta^+}^{\uparrow\downarrow}(x) &= 2d_{\Delta^+}^{\uparrow\downarrow}(x) = F_v(x) \pm \frac{1}{3}G_v(x) \\ u_{\Delta^+}^{\uparrow\uparrow}(x) &= 2d_{\Delta^+}^{\uparrow\uparrow}(x) = F_v(x) \pm G_v(x). \end{aligned} \quad (18)$$

On the other hand,  $SU(6)$  is broken for  $\Sigma^*$ . The up and/or down distributions in the  $\Sigma^*$  baryons have a maximum at  $x = 1 - m'_v/m_{\Sigma^*} = 1 - 1010/1385 \approx 0.27$  and the strange quark distributions at  $x = 1 - m_v/m_{\Sigma^*} = 1 - 850/1385 \approx 0.39$ . The quark distributions, for example, for the  $\Sigma^{*+}$  are given by the same expressions as those for  $\Delta^+$  replacing  $d$  by  $s$  and noting that the  $u$  distribution is to be calculated with the heavy diquark masses and the  $s$  distribution using the light diquark masses. Further, note that we have  $\Delta q^{3/2}(x) \equiv q^{\uparrow\uparrow}(x) - q^{\downarrow\downarrow}(x) = 3\Delta q^{1/2}(x) \equiv q^{\uparrow}(x) - q^{\downarrow}(x)$ . In Figs. 8 and 9 we show the unpolarized and polarized quark distributions in the  $\Delta^+$  and  $\Sigma^{*+}$ . The  $\Delta q$  are for the spin- $\frac{1}{2}$  projections. They have to be multiplied by 3 to obtain the corresponding distributions for the spin- $\frac{3}{2}$  projections. In

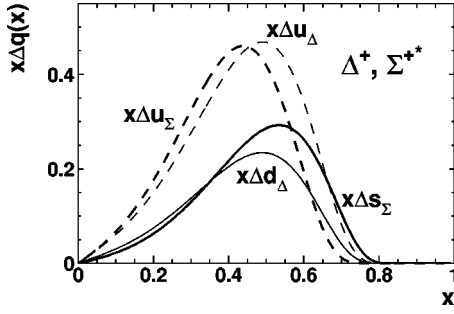


FIG. 9. Polarized quark distributions in the  $\Delta^+$  and  $\Sigma^{*+}$  at the bag scale,  $\mu^2$ .

Fig. 4, we show the ratio  $r_{\Sigma^*} \equiv s_{\Sigma^*}/u_{\Sigma^*}$  compared to the corresponding ratios in other hyperons.

### III. MESON CLOUD CORRECTIONS

The importance of the chiral structure of nucleons is well established both experimentally and theoretically. The pion-cloud associated with chiral symmetry breaking was first discussed in the context of deep-inelastic scattering by Feynman [12] and Sullivan [13]. It leads to flavor symmetry violation (FSV) in the sea-quark distributions of the nucleons, as realized by Thomas [14]. FSV in the proton was first observed experimentally by the New Muon Collaboration (NMC) through a violation of the Gottfried sum-rule [15]. More recently it has been directly studied by the NA51 Collaboration at CERN [16], by the E866 Collaboration at Fermilab [17] and by the Hermes Collaboration at Desy [18]. The role of the meson-cloud in understanding these data have been discussed extensively in the literature [19,20] — for recent reviews see Refs. [21–23]. On the other hand, relatively less attention has been paid to the effects of the meson-cloud in other baryons. As pointed out by Alberg *et al.*, and discussed in more detail in Ref. [24], the meson-cloud predicts an excess of  $\bar{d}$  over  $\bar{u}$  in  $\Sigma^+$  hyperons similar to that observed in protons, while SU(3) suggests  $\bar{d} < \bar{u}$ , since under  $p \leftrightarrow \Sigma^+$  we have  $s(\bar{s}) \leftrightarrow d(\bar{d})$ . The meson-cloud also modifies the bare quark distributions of the hyperons. In the following we discuss both FSV in hyperons and the modification of the bare quark distributions due to the meson-cloud.

In order to take account of the chiral structure of a baryon, its wave function is written as the sum of meson baryon Fock states

$$|H\rangle = \sqrt{Z}|H\rangle_{bare} + \sum_{BM} \int dy d^2\vec{k}_\perp \phi_{BM}(y, k_\perp^2) |B(y, \vec{k}_\perp)\rangle; \\ \times M(1-y, -\vec{k}_\perp)\rangle. \quad (19)$$

Here  $\phi_{BM}(y, k_\perp^2)$  is the probability amplitude for the hyperon to fluctuate into a virtual baryon-meson  $BM$  system with the baryon and meson having longitudinal momentum fractions  $y$  and  $1-y$  and transverse momenta  $\vec{k}_\perp$  and  $-\vec{k}_\perp$ , respec-

tively.  $Z$  is the wave function renormalization constant and is equal to the probability to find the bare hyperon in the physical hyperon.

In the following we discuss the chiral structure of the  $\Sigma^+$  as an example and compare it to that of the nucleons. The nucleon case has already been discussed in [25]. The extension to other baryons is straightforward. The lowest lying fluctuations for  $\Sigma^+$  which we include in our calculation are

$$\begin{aligned} \Sigma^+(uus) &\rightarrow \Lambda^0(uds)\pi^+(u\bar{d}) \\ \Sigma^+(uus) &\rightarrow \Sigma^0(uds)\pi^+(u\bar{d}) \\ \Sigma^+(uus) &\rightarrow \Sigma^+(uus)\pi^0\left(\frac{1}{\sqrt{2}}[d\bar{d}-u\bar{u}]\right) \\ \Sigma^+(uus) &\rightarrow \Sigma^{0*}(uds)\pi^+(u\bar{d}) \\ \Sigma^+(uus) &\rightarrow \Sigma^{*+}(uus)\pi^0\left(\frac{1}{\sqrt{2}}[d\bar{d}-u\bar{u}]\right) \\ \Sigma^+(uus) &\rightarrow p(uud)\bar{K}^0(\bar{d}s). \end{aligned} \quad (20)$$

The corresponding lowest fluctuations for the proton are

$$\begin{aligned} p(uud) &\rightarrow n(udd)\pi^+(u\bar{d}) \\ p(uud) &\rightarrow p(uud)\pi^0\left(\frac{1}{\sqrt{2}}[d\bar{d}-u\bar{u}]\right) \\ p(uud) &\rightarrow \Delta^+(uud)\pi^0\left(\frac{1}{\sqrt{2}}[d\bar{d}-u\bar{u}]\right) \\ p(uud) &\rightarrow \Delta^0(udd)\pi^+(u\bar{d}) \\ p(uud) &\rightarrow \Delta^{++}(uuu)\pi^-(\bar{u}d). \end{aligned} \quad (21)$$

Since the  $\Delta$  plays an important role in the nucleon, we also include the  $\Sigma^*\pi$  components of the wave function in the  $\Sigma^+$  case.

In deep inelastic scattering, the virtual photon can hit either the bare hadron,  $H$ , or one of the constituents of the higher Fock states. In the infinite momentum frame, where the constituents of the target can be regarded as free during the interaction time, the contribution of the higher Fock states to the quark distribution of the physical hadron,  $H$ , can be written as the convolution

$$\delta q_H(x) = \sum_{MB} \left[ \int_x^1 f_{MB/H}(y) q_M\left(\frac{x}{y}\right) \frac{dy}{y} \right. \\ \left. + \int_x^1 f_{BM/H}(y) q_B\left(\frac{x}{y}\right) \frac{dy}{y} \right], \quad (22)$$

where the splitting functions  $f_{MB/H}(y)$  and  $f_{BM/H}(y)$  are related to the probability amplitudes  $\phi_{BM}$  by

$$f_{BM/H}(y) = \int_0^\infty dk_\perp^2 |\phi_{BM}(y, k_\perp^2)|^2,$$

$$f_{MB/H}(y) = \int_0^\infty dk_\perp^2 |\phi_{BM}(1-y, k_\perp^2)|^2. \quad (23)$$

They can be calculated by using time-ordered perturbation theory in the infinite momentum frame. The quark distributions in a physical hadron,  $H$  are then given by

$$q_H(x) = Z q_H^{\text{bare}} + \delta q_H(x) \quad (24)$$

where  $q_H^{\text{bare}}$  are the bare quark distributions and  $Z$  is a renormalization constant which can be expressed as

$$Z \equiv 1 - \sum_{MB} \int_0^1 f_{MB/H}(y) dy. \quad (25)$$

These concepts can be extended to polarized particles by introducing the probability amplitudes  $\phi_{BM}^{\lambda\lambda'}(y, k_\perp)$  for a hadron with given positive helicity to be in a Fock state consisting of a baryon with helicity  $\lambda$  and meson with helicity  $\lambda'$ . The splitting functions are then given by

$$f_{BM/H}^\lambda(y) = \sum_{\lambda'} \int_0^\infty dk_\perp^2 |\phi_{BM}^{\lambda\lambda'}(y, k_\perp^2)|^2,$$

$$f_{MB/H}^{\lambda'}(y) = \sum_{\lambda} \int_0^\infty dk_\perp^2 |\phi_{BM}^{\lambda\lambda'}(1-y, k_\perp^2)|^2. \quad (26)$$

The contribution of higher Fock states to the polarized quark distributions,  $\Delta q_H(x) = q_H^\uparrow(x) - q_H^\downarrow(x)$ , are then

$$\Delta \delta q_H(x) = \sum_{MB} \left[ \int_x^1 \Delta f_{BM/H}(y) \Delta q_B \left( \frac{x}{y} \right) \frac{dy}{y} + \int_x^1 \Delta f_{MB/H}(y) \Delta q_M \left( \frac{x}{y} \right) \frac{dy}{y} \right], \quad (27)$$

where  $\Delta f_{BM/H}(y)$  and  $\Delta f_{MB/H}(y)$  are defined by  $\Delta f_{BM/H}(y) \equiv \sum_{\lambda\lambda'} 2\lambda f_{BM/H}^{\lambda\lambda'}(y)$  and  $\Delta f_{MB/H}(y) \equiv \sum_{\lambda\lambda'} 2\lambda' f_{MB/H}^{\lambda\lambda'}(y)$ , respectively. The contributions from the second term in Eq. (27) are zero for pseudoscalar mesons.

The amplitudes  $\phi_{BM}^{\lambda\lambda'}(y, k_\perp^2)$  may be expressed in the following form:

$$\phi_{BM}^{\lambda\lambda'}(y, k_\perp^2) = \frac{1}{2\pi\sqrt{y(1-y)}} \frac{\sqrt{m_H m_B} V_{IMF}^{\lambda\lambda'}(y, k_\perp^2)}{m_H^2 - \mathcal{M}_{BM}^2(y, k_\perp^2)}. \quad (28)$$

Here,  $V_{IMF}^{\lambda\lambda'}$  describes the vertex and contains the spin-dependence of the amplitude. The exact form of the  $V_{IMF}^{\lambda\lambda'}$  can be found for various transitions in Refs. [21] and [26]. Because of the extended nature of the vertices one

has to introduce phenomenological vertex form factors,  $G_{HBM}(y, k_\perp^2)$ , which parametrize the unknown dynamics at the vertices. These are often parametrized as

$$G_{HBM}(y, k_\perp^2) = \left( \frac{\Lambda_{BM}^2 + m_H^2}{\Lambda_{BM}^2 + \mathcal{M}_{BM}^2(y, k_\perp^2)} \right)^2, \quad (29)$$

where

$$\mathcal{M}_{BM}^2 = \frac{k_\perp^2 + m_B^2}{y} + \frac{k_\perp^2 + m_M^2}{1-y} \quad (30)$$

is the invariant mass of the meson-baryon fluctuation.

In calculating the matrix element of the axial-current or  $g_1$  in the meson-cloud model, one has to include terms in which the polarized photon-N (photon- $\Sigma$ ) interaction leads to the same final states as the polarized photon- $\Delta$  (photon- $\Sigma^*$ ) interaction [27]. The contributions of these interference terms to the measured quark distributions can be written as

$$\Delta \delta^{\text{int}} q_H(x) = \sum_{MB_1 B_2} \left[ \int_x^1 \Delta f_{(B_1 B_2)M/H}(y) \Delta q_{B_1 B_2} \left( \frac{x}{y} \right) \frac{dy}{y} + \int_x^1 \Delta f_{(M_1 M_2)B/H}(y) \Delta q_{M_1 M_2} \left( \frac{x}{y} \right) \frac{dy}{y} \right], \quad (31)$$

where the interference splitting functions are given by

$$\Delta f_{(B_1 B_2)M/H}(y) = \sum_{\lambda\lambda'} 2\lambda \int_0^\infty dk_\perp^2 \phi_{B_1 M}^{\lambda\lambda'}(y, k_\perp^2) \phi_{B_2 M}^{*\lambda\lambda'}(y, k_\perp^2)$$

$$\Delta f_{(M_1 M_2)B/H}(y) = \sum_{\lambda\lambda'} 2\lambda' \int_0^\infty dk_\perp^2 \phi_{M_1 B}^{\lambda\lambda'}(y, k_\perp^2) \phi_{M_2 B}^{*\lambda\lambda'}(y, k_\perp^2). \quad (32)$$

The interference distributions  $q_{B_1 B_2}$  and  $q_{M_1 M_2}$  in Eq. (31) do not have the same straightforward interpretation as quark distributions. They have to be modeled in some way. Using the  $SU(6)$  wave functions of the baryons from the baryon octet and decuplet, the transition matrix elements,  $\langle B_8 | P_{f,m} | B_8' \rangle$  and  $\langle B_8 | P_{f,m} | B_{10} \rangle$ , may be calculated and the interference distributions may be related to the quantities  $F_s$ ,  $F_v$ ,  $G_v$  and  $G_s$  calculated in the MIT bag. For the  $\Delta N$  interference terms we obtain

$$u_{\Delta^+ p}^{\uparrow\downarrow} = u_{\Delta^0 n}^{\uparrow\downarrow} = \pm \frac{\sqrt{2}}{3} G_v(x)$$

$$d_{\Delta^+ p}^{\uparrow\downarrow} = d_{\Delta^0 n}^{\uparrow\downarrow} = \mp \frac{\sqrt{2}}{3} G_v(x). \quad (33)$$



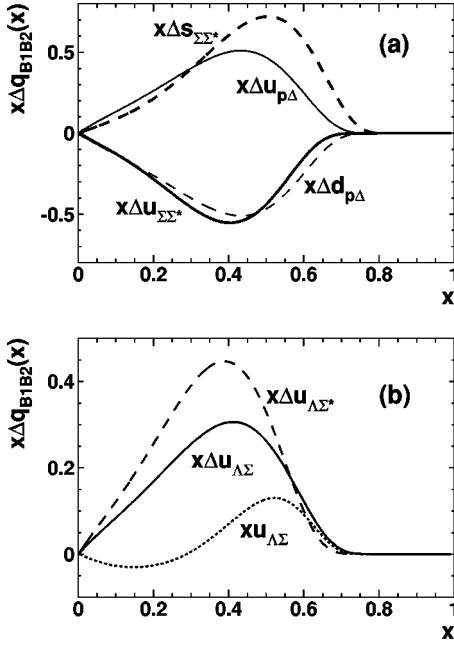


FIG. 10. Interference distributions as calculated in the MIT bag at the scale,  $\mu^2$ . (a)  $N$ - $\Delta$  and  $\Sigma$ - $\Sigma^*$  interference terms; (b)  $\Lambda$ - $\Sigma$  and  $\Lambda$ - $\Sigma^*$  interference terms. The  $d$  distributions have the same magnitude but opposite signs than the corresponding  $u$ -distributions.

The possible interference terms for the  $\Sigma^+$  are  $\Lambda$ - $\Sigma^0$ ,  $\Lambda$ - $\Sigma^{*0}$ ,  $\Sigma^0$ - $\Sigma^{*0}$  and  $\Sigma^+$ - $\Sigma^{*+}$ . We obtain for the  $\Lambda$ - $\Sigma^0$  interference

$$u_{\Lambda\Sigma^0}^{\uparrow\downarrow} = -d_{\Lambda\Sigma^0}^{\uparrow\downarrow} = \frac{\sqrt{3}}{8} [F'_s - F'_v] \pm \frac{\sqrt{3}}{8} \left[ G'_s + \frac{1}{3} G'_v \right]$$

$$s_{\Lambda\Sigma^0}^{\uparrow\downarrow} = 0, \quad (34)$$

for the  $\Lambda$ - $\Sigma^{*0}$  interference

$$u_{\Lambda\Sigma^{*0}}^{\uparrow\downarrow} = -d_{\Lambda\Sigma^{*0}}^{\uparrow\downarrow} = \pm \frac{1}{\sqrt{6}} G'_v(x)$$

$$s_{\Lambda\Sigma^{*0}}^{\uparrow\downarrow} = 0, \quad (35)$$

and for the  $\Sigma^0$ - $\Sigma^{*0}$  and  $\Sigma^+$ - $\Sigma^{*+}$  interference terms

$$u_{\Sigma^+\Sigma^+}^{\uparrow\downarrow} = 2u_{\Sigma^0\Sigma^0}^{\uparrow\downarrow} = 2d_{\Sigma^0\Sigma^0}^{\uparrow\downarrow} = \mp \frac{\sqrt{2}}{3} G'_v(x)$$

$$s_{\Sigma^+\Sigma^+}^{\uparrow\downarrow} = s_{\Sigma^0\Sigma^0}^{\uparrow\downarrow} = \pm \frac{\sqrt{2}}{3} G_v(x). \quad (36)$$

We use the average mass of the octet and decuplet baryons involved in the calculation of  $F_s$ ,  $F_v$ ,  $G_s$  and  $G_v$ . The results for  $p$ - $\Delta$  and  $\Sigma$ - $\Sigma^*$  are shown in Fig. 10a and those for  $\Lambda$ - $\Sigma^*$  and  $\Lambda$ - $\Sigma$  in Fig. 10b. The  $d$  distributions for the  $\Lambda$ - $\Sigma$  interference terms can be obtained by multiplying the corresponding  $u$  distributions by  $-1$ . Note that, if  $SU(6)$  is not a good symmetry, we have  $F_s \neq F_v$  and the  $\Lambda$ - $\Sigma^0$  inter-

ference also contributes to the the unpolarized  $u$  and  $d$  quark distributions. This is shown in Fig. 10b. However, the net contributions, i.e. the integral over  $u_{\Lambda\Sigma^0}$  and that over  $d_{\Lambda\Sigma^0}$ , are zero and baryon number conservation is not violated. Note also that the interference distributions for  $\Sigma$ - $\Sigma^*$  and  $N$ - $\Delta$  have opposite signs. Nevertheless, they contribute both positively to  $\Delta u$  since the splitting functions have opposite signs as we shall discuss below.

In order to calculate the meson cloud corrections to the quark distributions we have to specify the coupling constants and the cut-off parameters.  $SU(3)$  relates the coupling constants by  $g_{\Sigma\Sigma\pi} = 2(1-\alpha)g_{NN\pi}$ ,  $g_{\Sigma\Lambda\pi} = (2/\sqrt{3})\alpha g_{NN\pi}$ ,  $g_{\Sigma^+\pi\bar{K}^0} = \sqrt{2}(1-2\alpha)g_{NN\pi}$  and  $g_{\Sigma\Sigma^*\pi} = (1/\sqrt{6})g_{N\Delta\pi}$  where we defined  $g_{NN\pi} \equiv g_{pp\pi^0}$ ,  $g_{N\Delta\pi} \equiv g_{p\Delta^{++}\pi^-}$ ,  $g_{\Sigma\Sigma\pi} \equiv g_{\Sigma^+\Sigma^+\pi^0}$ , and  $g_{\Sigma\Sigma^*\pi} \equiv g_{\Sigma^+\Sigma^*\pi^0}$ .  $\alpha$  is defined by  $\alpha \equiv D/(D+F) \approx 0.635$  with  $D$  and  $F$  the symmetric and anti-symmetric  $SU(3)$  couplings. The numerical values are given by  $g_{pN\pi}^2/4\pi = 13.6$  and  $g_{p\Delta\pi}^2/4\pi = 11.08 \text{ GeV}^{-2}$  and the couplings of a given type of fluctuation with different isospin components are related by isospin Clebsch-Gordan coefficients, i.e.  $g_{pn\pi^+} = -\sqrt{2}g_{pp\pi^0}$ ,  $g_{p\Delta^0\pi^+} = -(1/\sqrt{2})g_{p\Delta^{++}\pi^0} = (1/\sqrt{3})g_{p\Delta^{++}\pi^-}$ ,  $g_{\Sigma^+\Sigma^0\pi^+} = -g_{\Sigma^+\Sigma^+\pi^0}$ , and  $g_{\Sigma^+\Sigma^{*0}\pi^+} = -g_{\Sigma^+\Sigma^*\pi^0}$ . The cut-off parameters may be determined in independent experiments, for example in inclusive particle production in hadron hadron collisions [21,28,29]. The violation of the Gottfried sum rule and of flavor symmetry puts also constraints on the magnitude of these parameters. They are also restricted by the requirement that the contributions from the meson cloud to the sea quark distributions cannot be larger than the measured sea quark distributions. The values,  $\Lambda_{MB} = 1.0 \text{ GeV}$  and  $\Lambda_{MB} = 1.3 \text{ GeV}$  for the  $\pi N$  and  $\pi\Delta$  components, respectively, give contributions to the  $\bar{u}$  and  $\bar{d}$  which are consistent with this requirement and also with FSV violation [20] (see below). Unfortunately, there is not much known about the cut-off parameters in the  $\Sigma^+$  case. In the absence of any information, we use the same values as in the proton case. With this choice of parameters the probabilities for the various fluctuations are approximately given by  $P_{N\pi/p} = 13\%$ ,  $P_{\Delta\pi/p} = 11\%$  and  $P_{\Sigma\pi/\Sigma} = 3.7\%$ ,  $P_{\Sigma^*\pi/\Sigma} = 3.1\%$ ,  $P_{\Lambda\pi/\Sigma} = 3.2\%$  and  $P_{p\bar{K}^0/\Sigma} = 0.4\%$ , respectively.

The spin averaged splitting functions for  $p \rightarrow BM$  and  $\Sigma^+ \rightarrow BM$  are shown in Fig. 11. Here, the splitting functions for a given type of fluctuation are defined as the sum over all isospin states - i.e.,  $f_{N\pi/p} \equiv f_{p\pi^0/p} + f_{n\pi^+/p}$ , etc. Because of the smaller coupling constants in the  $\Sigma^+$  case the meson-cloud is less important for the  $\Sigma^+$ . Further, the transition,  $\Sigma^+ \rightarrow \bar{K}^0 p$ , only plays a marginal role as can be seen in Fig. 11b. In calculating the meson-cloud corrections we use our bag model results for the bare distributions of the hyperons and nucleons. We also use a parametrization of the quark distributions in the pions [30] and utilize experimental data for the ratio  $\bar{u}^{K^-}/\bar{u}^{\pi^-} \sim (1-x)^{0.18 \pm 0.07}$  [31] to obtain the light quark valence distribution in the kaon. The strange quark distribution in the kaon is expected to be harder because of the mass of the strange quark. We use the param-

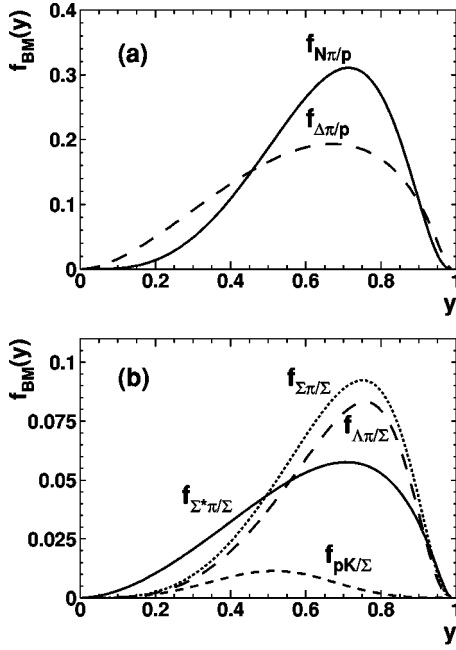


FIG. 11. Splitting functions for the transitions (a)  $p \rightarrow BM$  and (b)  $\Sigma^+ \rightarrow BM$ .

erization of Ref. [24] for the kaon quark distributions, which are constructed to satisfy the above requirements:

$$xu(x) = 1.05x^{0.61}(1-x)^{1.20},$$

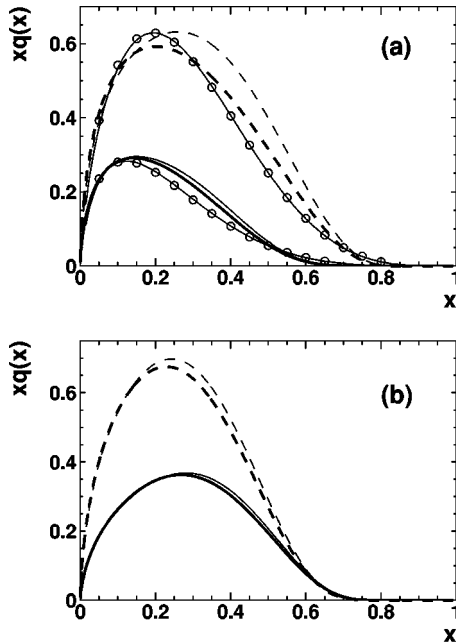


FIG. 12. (a) The up (dashed lines) and down (solid lines) valence quark distribution in the proton without (light lines) and with (heavy lines) meson-cloud corrections at  $Q^2 = 10 \text{ GeV}^2$ . The Cteq4M distributions representing the “data” are shown as solid lines with open circles. (b) The up (dashed lines) and strange (solid lines) valence quark distribution in the  $\Sigma^+$  without (light lines) and with (heavy lines) meson-cloud corrections at  $Q^2 = 10 \text{ GeV}^2$ .

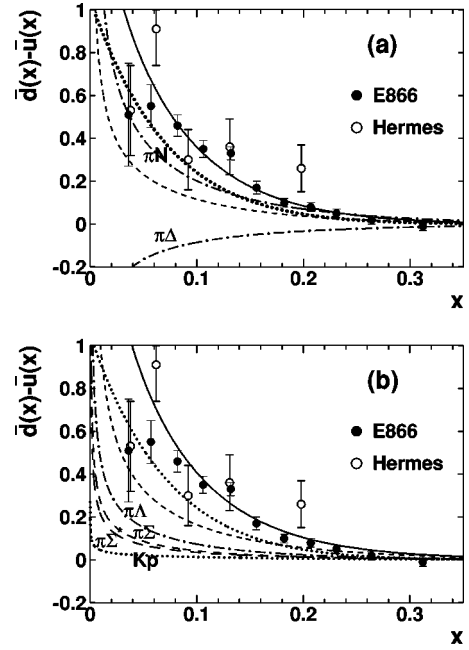


FIG. 13. Flavor symmetry violation,  $\bar{d} - \bar{u}$ , for (a) the proton and (b) the  $\Sigma^+$ . In the proton case, the upper and lower dash-dotted lines stand for the  $\pi N$  and  $\pi\Delta$  contributions alone and the dashed line for their sum. The data are taken from Refs. [17,18]. In the  $\Sigma^+$  case, the upper and lower dashed lines stand for the  $\pi\Sigma$  and  $\pi\Sigma^*$  contributions, the dotted line for the  $Kp$  and the dash-dotted line for the  $\pi\Lambda$  contributions—and the proton data is shown just to set the scale. The short dashed line is the sum of the chiral components. The dotted lines are the Pauli contributions and the solid lines stand for the total FSV.

$$xs(x) = 0.94x^{0.61}(1-x)^{0.86}. \quad (37)$$

First, we show the modifications of the bare valence quark distributions in the proton and in the  $\Sigma^+$  in Fig. 12. We see that the meson-cloud plays a relatively more important role in the proton than in the  $\Sigma^+$ . The strange to light quark ratio,  $r_\Sigma = s_\Sigma / u_\Sigma$ , is not sensitive to meson-cloud corrections, as shown in Fig. 4.

The meson cloud model predicts flavor symmetry violations not only for the proton but also for other baryons. Since  $p \leftrightarrow \Sigma^+$  means  $d(\bar{d}) \leftrightarrow s(\bar{s})$  under  $SU(3)$ , one would expect an excess of  $\bar{s}$  over  $\bar{u}$  on the basis of complete  $SU(3)$  symmetry and the measured FSV in the proton. However, in the meson-cloud model,  $s\bar{s}$  fluctuations for the  $\Sigma^+$  involve hyperons containing at least two strange quarks,  $\Xi$ 's, and are strongly suppressed due to the higher masses of these hyperons, which is of course a direct consequence of  $SU(3)$  breaking. On the other hand, meson-cloud contributions lead to an excess of  $\bar{d}$  over  $\bar{u}$  for the  $\Sigma^+$ , as can be seen in Eq. (20). This FSV is not at all related to  $SU(3)$  symmetry. Furthermore, FSV could be even larger in the  $\Sigma^+$  case since here *all* fluctuations contribute to  $\bar{d}$ . We show the calculated FSV violation for the proton in Fig. 13a and for the  $\Sigma^+$  in Fig.

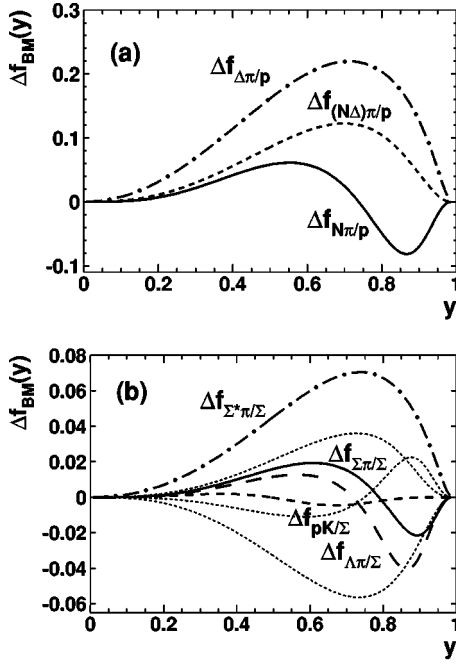


FIG. 14. The polarized splitting functions for the transitions (a)  $p \rightarrow BM$  and (b)  $\Sigma^+ \rightarrow BM$ . The dotted lines are the interference splitting functions;  $\Delta f_{(\Lambda\Sigma^*)\pi/\Sigma}$  (upper line),  $\Delta f_{(\Lambda\Sigma)\pi/\Sigma}$  (middle line) and  $\Delta f_{(\Sigma\Sigma^*)\pi/\Sigma}$  (lower line).

13b, together with the E866 data for the proton. For the proton, the upper and lower dash-dotted curves are the contributions from the  $\pi N$  and the  $\pi\Delta$  components alone and the dashed curve is the sum of  $\pi N$  and  $\pi\Delta$ .

As pointed out in Ref. [20], the measured  $x$ -dependence of the FSV, especially that of the ratio  $\bar{d}/\bar{u}$  (not shown), requires a relatively large contribution from the  $\Delta\pi$  component in the proton case, which cancels the contributions from the  $N\pi$  component at large  $x$  values and leads to the required fast decrease of the asymmetry in this region. Since, on the other hand, the magnitude of the  $N\pi$  and  $\Delta\pi$  components are restricted by the requirement that their contributions to the total sea quark distributions cannot be larger than the experimentally measured value, an additional non-chiral component is needed at small  $x$ . This non-chiral component may be attributed to the Pauli exclusion principle, as suggested by Field and Feynman [32]. Because of the Pauli

exclusion principle, the presence of two valence  $u$  quarks in the proton, as opposed to a single valence  $d$  quark, makes it less probable to produce a  $u\bar{u}$  pair compared to a  $d\bar{d}$  pair giving an excess of  $\bar{d}$  over  $\bar{u}$  in the non-perturbative sea. Based on bag model calculations [4], it is expected that this component should have a shape similar to the usual sea quark distributions, contributing to the asymmetry at lower  $x$  values than the chiral component. Since we have two valence  $u$  quarks and no  $d$  valence quarks in the  $\Sigma^+$  we expect that the component arising from the Pauli principle will be at least as large as that in the proton case. [Neglecting SU(3) breaking one would expect it to be twice as large for the  $\Sigma^+$  as for the proton.] The Pauli contributions are shown as the dotted line and the sum of the chiral and Pauli components as solid lines in Figs. 13a and 13b. In the  $\Sigma^+$  case, we show also the contributions from the various meson baryon fluctuations, the upper and lower dashed curves stand for the  $\pi\Sigma$  and  $\pi\Sigma^*$  contributions, the dotted line for the  $Kp$  and the dash-dotted for the  $\pi\Lambda$  contribution. The sum of all chiral contributions is shown as the short dashed line. Note that, while the contribution of the  $\pi\Delta$  component is negative in the proton case, the  $\pi\Sigma^*$  component reinforces the FSV in the  $\Sigma^+$  case giving rise to as large a FSV as in the proton case — even though the total meson-cloud corrections are less important for the  $\Sigma^+$ .

Since the pseudoscalar mesons do not contribute to the spin dependent quark distributions of the baryons, the meson-cloud corrections decrease the amount of the baryon spin carried by the spin of the quarks. The polarized splitting functions for the proton and  $\Sigma^+$  are shown in Figs. 14a and 14b, respectively. (Note that, according to the definition, the decuplet splitting functions are the sum of the 3/2 and 1/2 helicity components with the 3/2 component multiplied by a factor of 3.) Since the fluctuations involving baryons from the octet are positive for small  $y$  values and negative for larger  $y$  values, their contribution to the spin of the nucleon or hyperon is relatively small. The integral,  $\langle \Delta f_{N\pi/p} \rangle \approx 0.01$ , nearly vanishes. On the other hand, the splitting functions of the baryons from the baryon decuplet are positive over the whole  $y$  region and their contributions are much larger,  $\langle \Delta f_{\Delta\pi/p} \rangle \approx 0.11$ . These values are to be compared to the values  $\langle f_{N\pi/p} \rangle = 0.13$  and  $\langle f_{\Delta\pi/p} \rangle = 0.11$  which can be roughly thought of as the amount of spin “lost” through the meson baryon fluctuation. (Remember that mesons do not contrib-

TABLE I. Fraction of angular momentum carried by the spin of the quarks in different models.  $\Delta Q \equiv \Delta q + \Delta \bar{q}$ . The results in the third row are obtained by using  $\Sigma = 0.28$  from deep inelastic scattering (DIS) experiments,  $F + D = 1.2573$  and  $F/D = 0.575$  from hyperon decay experiments.

Model	proton				$\Sigma^+$			
	$\Delta U$	$\Delta D$	$\Delta S$	$\Sigma$	$\Delta U$	$\Delta D$	$\Delta S$	$\Sigma$
NQM	4/3	-1/3	0	1	4/3	0	-1/3	1
DIS+SU(3)	0.82	-0.44	-0.10	0.28	0.82	-0.10	-0.44	0.28
Bag	1.05	-0.26	0	0.79	1.05	0	-0.27	0.78
Bag+MC	0.86	-0.17	<0.01	0.69	0.93	<0.01	-0.24	0.69
Bag+MC+IF	0.94	-0.25	<0.01	0.69	0.98	<0.01	-0.28	0.70

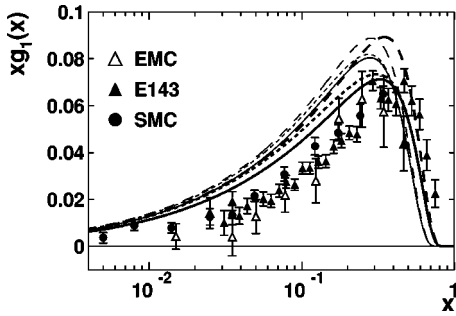


FIG. 15.  $g_{1\Sigma^+}$  with (light solid line) and without (light dashed line) meson-cloud corrections compared to the corresponding  $g_{1p}$  (heavy lines). The data are for the proton and taken from Refs. [33–35]. The structure functions calculated with interference terms are shown as short dashed lines. The EMC data are at different  $Q^2$  values, the SMC at  $Q^2=10$  GeV<sup>2</sup> and the E143 data at  $Q^2=5$  GeV<sup>2</sup>.

ute to the spin of the nucleon.) The splitting functions corresponding to interference between octet and decuplet baryons (short dashed lines) are positive. However, since the interference distributions for  $d$  and  $s$  quarks are opposite in sign to the  $u$  distributions (see Fig. 10) they approximately cancel each other in the “spin sum.” On the other hand, they contribute positively to  $g_1$  since, here, the  $u$  distributions are weighted by  $4/9$  as opposed to  $1/9$  of the  $d$  and  $s$  distributions.

In Table I, we show spin fractions carried by the different flavors of the proton and the  $\Sigma^+$ ,  $\Delta Q \equiv \Delta q + \Delta \bar{q}$ , in the non-relativistic quark model (NQM), as measured in DIS and using  $SU(3)$  symmetry to obtain the values for  $\Sigma^+$  [DIS+ $SU(3)$ ], in the bag model, in the bag model with meson cloud corrections (bag+MC) and with interference terms (IF).  $\Delta S$  in the proton comes from the  $\Lambda K$  and  $\Sigma K$  component of the wave function. However, these give very small contributions.  $\Delta D$  in the  $\Sigma^+$  comes from lower lying fluctuations and could be sizable. However, because the integral over the splitting function for the octet baryons approximately vanishes, it is very small ( $<1\%$ ). Here, the interference terms largely cancel each other. Further, we see that, because of the transverse motion of the quarks, the fraction of the spin carried by the quarks in the bag model is smaller than one. In conclusion, the meson cloud is responsible for part of the dilution of the spin though the fraction of spin carried by the quarks is still considerably larger than the experimental value.

In Fig. 15,  $xg_1(x)$  calculated for proton (heavy lines) and for  $\Sigma^+$  (light lines) are shown with (solid lines) and without (dashed lines) meson corrections and with interference terms (short dashed lines). The predictions for  $g_{1\Sigma^+}$  and  $g_{1p}$  are similar, with  $g_{1\Sigma^+}$  peaking at slightly lower  $x$ -values than  $g_{1p}$ . This is because the  $u$  quarks, which have a somewhat softer distribution in the  $\Sigma^+$  than in the proton, dominate in  $g_1$ .

In concluding this section we must issue a caution concerning the discussion of spin-dependent parton distributions here. It is by now well understood that the axial anomaly plays a vital role in the flavor singlet spin structure [36] and the model which we have used has not incorporated such effects. As a result the integral of  $g_{1p}$ , for example, satisfies the Ellis-Jaffe sum rule—with the octet and isovector axial charges appropriate to the model, including meson corrections. It is therefore not too surprising that our curves for  $g_{1p}$  lie above the data. A reasonable polarized gluon distribution could bring the calculated values in Table I into better agreement with the experimental value of  $\Sigma$ .

#### IV. CONCLUSIONS

We calculated the quark distribution functions of different hyperons in the MIT bag model using the approach of the Adelaide group which assures the correct support of the distribution functions. The hyperfine splitting responsible for the splitting of the masses of the  $N$ - $\Delta$ ,  $\Lambda$ - $\Sigma^0$  and  $\Sigma$ - $\Sigma^*$  results in quark distributions very different from  $SU(6)$  expectations. This  $SU(6)$  breaking goes beyond the explicit breaking through the strange quark mass and leads to different shapes of the quark distributions, even in hyperons with the same number of (valence) strange quarks. The strange to  $u$  ratio in the  $\Sigma^+$  increases with  $x \rightarrow 1$ —a behavior opposite to that predicted by  $SU(3)$ . Further, we predict polarized  $u$  and  $d$  quarks distributions in the  $\Lambda$  as a function of  $x$ , even though their net contributions to the total spin of the  $\Lambda$  are zero. This prediction could be tested in semi-inclusive polarized DIS since the coupling of the  $u$  quarks to the electromagnetic current is four times larger than that of the strange quarks.

We also calculated the modifications of the bare quark distributions through the meson-cloud required by chiral symmetry. Although the meson-cloud corrections to the distributions in the  $\Sigma^+$  are not as large as those to the corresponding distributions in the proton, because of the smaller coupling constants, the meson-cloud also leads to significant flavor symmetry violations in the sea quark distribution of the hyperons. We found that the  $\bar{d}$  in the  $\Sigma^+$  is enhanced relative to the  $\bar{u}$ , contrary to  $SU(3)$  expectations. The  $\bar{d}_{\Sigma^+}/\bar{u}_{\Sigma^+}$  ratio is comparable to the corresponding ratio  $\bar{d}_p/\bar{u}_p$  in the proton since, in the  $\Sigma^+$  case, all of the lowest lying fluctuations enhance the  $\bar{d}$  relative to  $\bar{u}$ .

#### ACKNOWLEDGMENTS

We would like to thank S. Braendler, W. Melnitchouk, A.W. Schreiber, F. Steffens and K. Tsushima for many useful conversations. This work was partly supported by the Australian Research Council.

- [1] M. Alberg *et al.*, Phys. Lett. B **389**, 367 (1996).  
[2] R. L. Jaffe, Nucl. Phys. **B229**, 205 (1983).  
[3] A. I. Signal and A. W. Thomas, Phys. Lett. B **211**, 481 (1988); Phys. Rev. D **40**, 2832 (1989); A. W. Schreiber *et al.*, *ibid.* **42**, 2226 (1990).  
[4] A. W. Schreiber, A. I. Signal, and A. W. Thomas, Phys. Rev. D **44**, 2653 (1991).  
[5] F. E. Close and A. W. Thomas, Phys. Lett. B **212**, 227 (1988).  
[6] H. L. Lai *et al.*, Phys. Rev. D **55**, 1280 (1997).  
[7] M. Miyama and S. Kumano, Comput. Phys. Commun. **94**, 185 (1996); M. Hirai, S. Kumano, and M. Miyama, *ibid.* **108**, 38 (1998).  
[8] J. J. de Swart, Rev. Mod. Phys. **35**, 916 (1963).  
[9] R. L. Jaffe, Phys. Rev. D **54**, 6581 (1996).  
[10] V. N. Gribov and L. N. Lipatov, Phys. Lett. **37B**, 78 (1971).  
[11] S. J. Brodsky and B.-Q. Ma, Phys. Lett. B **392**, 452 (1997).  
[12] R. P. Feynman, *Photon-Hadron Interactions* (W.A. Benjamin, New York, 1972).  
[13] J. D. Sullivan, Phys. Rev. D **5**, 1732 (1972).  
[14] A. W. Thomas, Phys. Lett. **126B**, 97 (1983).  
[15] P. Amaudruz *et al.*, Phys. Rev. Lett. **66**, 2712 (1991); Phys. Lett. B **292**, 159 (1992).  
[16] NA51 Collaboration, A. Baldit *et al.*, Phys. Lett. B **332**, 244 (1994).  
[17] E866 Collaboration, E. A. Hawker *et al.*, Phys. Rev. Lett. **80**, 3715 (1998).  
[18] Hermes Collaboration, K. Ackerstaff *et al.*, Phys. Rev. Lett. **81**, 5519 (1998).  
[19] E. M. Henley and G. A. Miller, Phys. Lett. B **251**, 453 (1990); A. I. Signal, A. W. Schreiber, and A. W. Thomas, Mod. Phys. Lett. A **6**, 271 (1991); S. Kumano, Phys. Rev. D **43**, 3067 (1991); S. Kumano and J. T. Londergan, *ibid.* **44**, 717 (1991).  
[20] W. Melnitchouk, J. Speth, and A. W. Thomas, Phys. Rev. D **59**, 014033 (1999).  
[21] J. Speth and A. W. Thomas, Adv. Nucl. Phys. **24**, 83 (1998).  
[22] J. T. Londergan and A. W. Thomas, Prog. Part. Nucl. Phys. **41**, 49 (1998).  
[23] S. Kumano, Phys. Rep. **303**, 103 (1998).  
[24] M. Alberg, T. Falter, and E. M. Henley, Nucl. Phys. **A644**, 93 (1998).  
[25] A. W. Schreiber *et al.*, Phys. Rev. D **45**, 3069 (1992); F. M. Steffens, H. Holtmann, and A. W. Thomas, Phys. Lett. B **358**, 139 (1995).  
[26] H. Holtmann, A. Szczurek, and J. Speth, Nucl. Phys. **A596**, 631 (1996).  
[27] A. W. Schreiber and A. W. Thomas, Phys. Lett. B **215**, 141 (1988).  
[28] V. R. Zoller, Z. Phys. C **54**, 425 (1992); **60**, 141 (1993).  
[29] C. Boros, Phys. Rev. D **59**, 051501 (1999).  
[30] M. Glück, E. Reya, and A. Vogt, Z. Phys. C **53**, 651 (1992).  
[31] J. Badier *et al.*, Phys. Lett. **93B**, 354 (1980).  
[32] R. D. Field and R. P. Feynman, Phys. Rev. D **15**, 2590 (1977).  
[33] EMC Collaboration, J. Ashman *et al.*, Nucl. Phys. **B328**, 1 (1989).  
[34] SMC Collaboration, B. Adeva *et al.*, Phys. Lett. B **412**, 414 (1997).  
[35] E143 Collaboration, F. Abe *et al.*, Phys. Rev. D **58**, 112004 (1998).  
[36] G. Altarelli and G. G. Ross, Phys. Lett. B **212**, 391 (1988); R. D. Carlitz, J. C. Collins, and A. H. Mueller, *ibid.* **214**, 299 (1988); A. V. Efremov, J. Soffer, and O. V. Teryaev, Nucl. Phys. **B246**, 97 (1990).